a more complete theoretical treatment of the Kondo problem. What we have demonstrated is that Eqs. (1) and (3) predict a susceptibility which agrees with experiment. If the theoretical assertions turn out to be incorrect, then Eqs. (1) and (2) are at least useful for representing data, i.e., as an empirical equation of state for this system. Work is in progress to see if the magnetic and thermal properties of any other Kondo system can be accounted for by this model.

†Based on work performed under the auspices of the U. S. Atomic Energy Commission.

[1]J. L. Tholence and R. Tournier, Phys. Rev. Lett. 25, 867 (1970).
[2]T. Sugawara and H. Eguchi, J. Phys. Soc. Jap. 26, 1322 (1969).
[3]A. S. Edelstein, Phys. Rev. Lett. 20, 1348 (1968).
[4]M. D. Daybell, W. P. Pratt, Jr., and W. A. Steyert, Phys. Rev. Lett. 22, 401 (1969).
[5]E. C. Hirschkoff, O. G. Symko, and J. C. Wheatley, private communication.
[6]R. Hasegawa and C. C. Tsuei, Phys. Rev. B 2, 1631 (1970).
[7]A. S. Edelstein, J. E. Jackson, and D. I. Bardos, in Proceedings of the International Conference in Magnetism, Grenoble, France, 1970 (to be published).
[8]A. S. Edelstein, Phys. Lett. 27A, 614 (1968).
[9]R. O. Elliott, H. H. Hill, and W. N. Miner, Phys. Status Solidi 32, 609 (1969).
[10]K. H. J. Buschow and H. J. van Daal, Phys. Rev. Lett. 23, 408 (1969).
[11]B. Coqblin and A. Blandin, Advan. Phys. 17, 281 (1968).
[12]P. W. Anderson, Phys. Rev. 164, 352 (1967).
[13]J. R. Schrieffer and P. A. Wolff, Phys. Rev. 149, 491 (1966).
[14]P. E. Bloomfield, R. Hecht, and P. R. Sievert, private communication. They have also included magnetic effects but their numerical results are not complete enough to allow detailed comparison with our work.
[15]P. W. Anderson, private communication.
[16]A. rough approximation for Eq. (3) is $\chi(T) \propto (k^2T^2 + \mu^2H^2 + \Delta^2)^{-1/4}$.
[17]B. N. Ganguly and C. S. Shastry, J. Phys. C: Proc. Phys. Soc., London 3, 1587 (1970).
[18]It should be observed that if $\Delta \approx kT_K$ for some system then $\chi(T,H) \propto (T_K)^{-1}[1-\frac{1}{3}(\pi T/2T_K)^2 - (\mu H/2kT_K)^2]$ for μH and $kT \ll kT_K$.

Mechanism of the Ferroelectric Phase Transformation in Rare-Earth Molybdates*

J. D. Axe, B. Dorner,† and G. Shirane
Brookhaven National Laboratory, Upton, New York 11973
(Received 14 January 1971)

Neutron scattering experiments on $Tb_2(MoO_4)_3$ show the ferroelectric orthorhombic phase to result from a phonon instability at the $(\frac{1}{2}, \frac{1}{2}, 0)$ Brillouin zone corner of the parent tetragonal phase. Anharmonic coupling to these antiferroelectric displacements produces a spontaneous strain which in turn causes a spontaneous polarization through normal piezoelectric coupling. The rare-earth molybdates thus represent a new class of displacive ferroelectric materials *without* a soft *polar* mode.

Borchardt and Bierstedt[1] have shown that $Gd_2(MoO_4)_3$ and the isostructural molybdates of Sm, Eu, Tb, and Dy all undergo ferroelectric phase transformations with transformation temperatures $150°C < T_0 < 190°C$. Subsequent investigations of the dielectric, optical, and mechanical behavior of these materials have revealed several unique and potentially useful properties.[2] The appearance of a spontaneous strain u_s coincident with the spontaneous polarization P_s, coupled with the fact that P_s, u_s states of opposite polarity can be induced by either applied electric fields or mechanical stress, has caused the term ferroelastic to be applied to these materials. There is a small anomalous contribution to the dielectric response of an *unclamped* crystal which appears abruptly upon passing from the higher temperature paraelectric (PE) phase to the ferroelectric (FE) phase and disappears with decreasing temperature. But, remarkably for a ferroelectric substance, this anomalous dielectric contribution disappears when the crystal is *clamped*.[2-4] These observations led Cross, Fouskova, and Cummins[3] to suggest that the transformation is driven by an *elastic instability* and that the P_s is an incidental but necessary consequence of the resulting u_s since the parent PE structure is piezoelectric.

Although this proposal is successful in explaining the apparent "clamping" of the dielectric behavior, it is not entirely satisfying because one should expect that the proposed elastic instability

is anticipated in the PE phase by a temperature-dependent decrease in the elastic stiffness, and this is not observed. In a recent note, Pytte[5] proposed an alternative mechanism in which the essential driving instability is not with respect to a homogeneous elastic deformation but rather involves atomic displacements associated with a normal phonon mode with finite wave vector $\vec{q}$. In this model both P_s and u_s then arise indirectly as a result of anharmonic coupling of these displacements with $\vec{q}=0$ optic and acoustic phonon displacements. We report here on neutron scattering experiments which completely confirm the essential features of Pytte's proposal, remove the existing uncertainties in the model, and allow us to formulate it in such a way as to exhibit simply the bistable nature of the electrical and elastic properties of these materials.

Our study was carried out at the Brookhaven high-flux beam reactor with an essentially single-crystal boule ($1\times1\times3$ cm^3) of $Tb_2(MoO_4)_3$ (TMO), chosen rather than the more extensively studied Gd compound (GMO) because of more favorable neutron scattering properties. A preliminary investigation of the sizes of the PE and FE unit cells was made by elastic scattering. This is of fundamental importance in understanding the transformation and the existing literature is contradictory.[4,6-9] We were able to index all observed FE reflections using an orthorhombic cell with $a_{FE}\approx b_{FE}\approx 10.4$ Å and $c_{FE}\approx 10.7$ Å. In particular, no evidence for enlargement in the a-b plane as reported by Drobyshev *et al*,[8] nor for doubling along the c axis reported under certain conditions by Kvapil and John,[9] was observed. In the PE phase a tetragonal cell of half the volume, with $a_{PE}\approx a_{FE}/\sqrt{2}$ and rotated by 45° in the FE a-b plane and with $c_{PE}\approx c_{PE}$, was adequate to index all observed reflections.[10] *Neither elastic nor* $\vec{q}=0$ *optical phonon instabilities can explain this doubling of the unit cell volume.*

The reduction in the translational symmetry necessary to pass from PE to FE phase must result from displacements modulated with the wave vector $\vec{q}_M=(\pi/a_{PE},\pi/a_{PE},0)$. These displacements give rise to new Bragg reflections ("superlattice" reflections) in the FE phase with reciprocal lattice vectors $\vec{G}_{hkl}+\vec{q}_M$, where $\vec{G}_{hkl}$ is a reciprocal lattice vector of the PE phase (see the insert of Fig. 1). The temperature dependence near T_0 of the elastic scattering intensity of two such superlattice reflections is shown in Fig. 1. The abrupt and nearly complete disappearance of intensity establishes $T_0=160\pm1$°C,

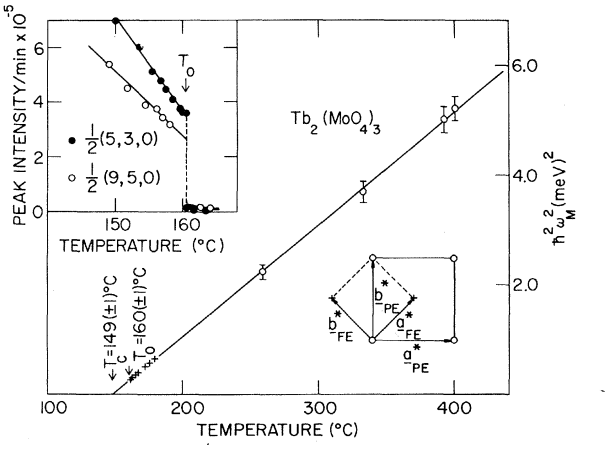

FIG. 1. Temperature dependence of the energy of the lowest lying phonon at the M point, $\vec{q}_M=(2\pi/a_{PE})(\frac{1}{2},\frac{1}{2},0)$. At higher temperatures ω_M was determined by fitting the spectral profiles (see Fig. 2). Near T_0 (crosses), $\omega_M(T)$ was determined from the temperature dependence of the integrated scattering intensity. The insert at the upper left shows the temperature dependence of two superlattice reflections near T_0. The insert at lower right is an $(hk0)$ section of the reciprocal lattice showing the normal (circles) and superlattice reflections (crosses).

in good agreement with published values,[1,4] and emphasizes the discontinuous (first-order) nature of the transformation. This latter result is in agreement with careful measurements of P_s as a function of T by Cummins[2] on GMO.

The remaining observations were concerned with the scattering which persists into the PE phase, and which can be seen as a high temperature tail in Fig. 1. This scattering intensity remains strongly localized around positions in reciprocal space where the FE superlattice reflections appear, and because the intensity is particularly strong at the reciprocal lattice point $(4,2,0)+(\frac{1}{2},\frac{1}{2},0)=\frac{1}{2}(9,5,0)$, this point was singled out for futher study. Figure 2 shows an energy analysis of this scattering performed on a three-axis crystal spectrometer.[11] Unlike the true Bragg scattering that exists below T_0, the scattering above T_0 shows appreciable inelasticity which increases as the temperature is raised, developing finally into well-defined but broadened peaks. This behavior is characteristic of the renormalization and gradual undamping of an unstable phonon mode, as has been observed to lead to structural transformations in several perovskite compounds.[12] The spectral profile is proportional to the product of a spectral correlation function $A(\omega)$, which we approximate with the familiar damped oscillator form, and a

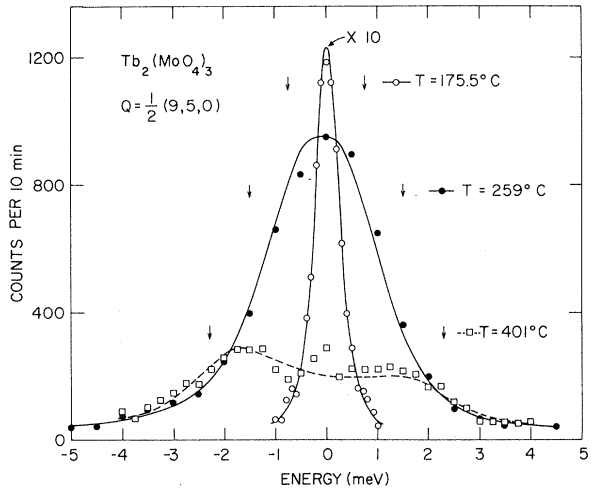

FIG. 2. Energy profile of scattering at a superlattice point in the PE phase, showing the evolution from underdamped phonon to strongly overdamped critical scattering as the temperature approaches T_c. The curves through the points are of the form of Eq. (1) modified by an approximate instrumental correction to account for asymmetry. The arrows indicate the values of $\omega_M(T)$ estimated by this fitting procedure.

thermal amplitude $[1+n(\omega)]$:

$$[1+n(\omega)]A(\omega)=\frac{k_B T\Gamma}{(\omega_M{}^2-\omega^2)^2+\omega^2\Gamma^2}, \tag{1}$$

if the energy transfer $\hbar\omega \ll k_B T$.

Making approximate corrections for instrumental effects, Eq. (1) accounts reasonably well for the observed line profiles at higher temperatures and allows us to extract values for the quasiharmonic frequency ω_M and damping parameter Γ as a function of temperature.[13] As shown in Fig. 1, $\omega_M(T)$ is consistent with

$$(\hbar\omega_M)^2=A(T-T_c) \tag{2}$$

which approximately characterizes all known soft-mode behavior,[14] with $A=(2.05\pm0.08)\times10^{-2}$ meV^2/°C and $T_c=149\pm2$°C. Γ was found to be $\sim2.5\pm0.3$ meV and nearly independent of temperature. At lower temperatures resolution effects make it increasingly difficult to determine ω_M from the line shape. Much less sensitive to resolution effects is the total scattered intensity, which, by integrating Eq. (1) over ω, is found to be independent of Γ and proportional to $T\omega_M{}^{-2}$. Using this result we have also established (crosses in Fig. 1) the validity of Eq. (2) in the temperature region just above T_0.[15] The fact that T_c lies ~10°C below T_0 again confirms the first-order nature of the transformation, although it is clear from the relative smallness of $(T_0-T_c)/T_0$, or equivalently the pronounced critical enhancement of the soft-mode fluctuations above T_0, that the transformation is "nearly" of second order.

We have thus established that the principal feature of Pytte's[5] model of the phase transformation, namely the existence of "soft"-phonon modes with $\vec{q}\neq0$, is correct. Pytte went on to establish a plausible mechanism for the observed macroscopic dielectric and elastic properties with the help of a phenomenological free-energy function describing both the PE and FE phases.[16,17] Pytte's final expressions, however, refer to only one of two possible polar phases. We think it is instructive to retain a complete set of order parameters (see below) in order to exhibit explicitly ferroelectric states of both polarities.

Following Miller and Kwok,[18] we describe the antiferroelectric component of the spontaneous internal atomic displacements in terms of the amplitudes $Q_\mu=(Q_{Mx},Q_{My})$ of a doubly degenerate[5] set of condensed normal phonon modes of wave vector $\vec{q}_M$,

$$\vec{u}(l\kappa)=\sum_\mu Q_\mu \xi_\mu(\kappa)\exp i(\vec{q}_M\cdot\vec{R}_{l\kappa}),$$

where $\vec{u}(l\kappa)$ is the displacement of the κth atom in the lth unit cell with position vector $\vec{R}_{l\kappa}$, and $\vec{\xi}_\mu(\kappa)$ is the (suitably normalized) phonon eigenvector of the μth mode. The Q_μ, supplemented with the macroscopic spontaneous strain tensor $u_{\alpha\beta}$, and polarization vector P_α serve as order parameters in the expansion of the free-energy function. We postulate it to be of the form[19]

$$F=[\tfrac{1}{2}\omega_M{}^2(Q_{Mx}{}^2+Q_{My}{}^2)+\tfrac{1}{4}V_4(Q_{Mx}{}^4+Q_{My}{}^4)+\tfrac{1}{2}V_4'Q_{Mx}{}^2Q_{My}{}^2+\cdots]+(\tfrac{1}{2}c_{66}{}^P u_{xy}{}^2+\tfrac{1}{2}\chi_{33}{}^{-1}P_z{}^2+\cdots)$$
$$+(g_{66}Q_{Mx}Q_{My}u_{xy}+a_{36}P_z u_{xy}+\cdots). \tag{3}$$

The bracketed terms represent the "harmonic" and higher-order contributions due to condensation of the degenerate phonon modes with $\vec{q}=\vec{q}_M$. The coefficient of the leading term is the square of the PE quasiharmonic mode frequency given by Eq. (2). Thus $\omega_M{}^2$ passes through zero at $T=T_c$.[18] Since $\vec{q}_M=0$, odd powers of Q_M are incompatible with the translational invariance of F.[18] There are two fourth-order terms which have the required symmetry invariance. The first parenthesis gives, respectively, the elastic energy of an x,y shear distortion of the lattice and the energy required for condensation of

a $\vec{q}=0$ optic phonon. χ_{33} is the clamped-dielectric susceptibility.

The first term of the last parenthesis is the lowest-order allowed coupling of Q_M with the strain. The last term is the normal piezoelectric coupling between u_{xy} and P_z. If we take the coefficients in the expansion, with the exception of ω_M^2, to be temperature independent, the elastic and dielectric properties of the tetragonal phase are temperature independent and "normal." To find the states which minimize F, we first set $\partial F/\partial P_z = \partial F/\partial u_{xy} = 0$, obtaining successively

$$P_z = -(a_{36}\chi_{33})u_{xy}, \tag{4a}$$

$$u_{xy} = -(g_{66}/c_{66}^{E})Q_{Mx}Q_{My}, \tag{4b}$$

where $c_{66}^{E} = c_{66}^{P} - a_{36}^{2}\chi_{33}$. Substituting these results into Eq. (3) gives

$$F = \tfrac{1}{2}\omega_M^2(Q_{Mx}^2+Q_{My}^2)+\tfrac{1}{4}V_4(Q_{Mx}^4+Q_{My}^4) + \tfrac{1}{2}[V_4' - (g_{66}^2/c_{66}^{E})]Q_{Mx}^2Q_{My}^2+\cdots. \tag{5}$$

Depending upon the values of V_4 and V_4', Eq. (5) can describe either first- or second-order transformations, as shown in Fig. 3. For simplicity we consider only second-order solutions, thereby avoiding the necessity of considering higher-order terms.

(1) $\omega_M^2 > 0$ (i.e., $T > T_c$). The stable solutions ($Q_{Mx} = Q_{My} = u_{xy} = P_z = 0$) correspond to the PE phase.

(2) $\omega_M^2 < 0$; $V_4' > (V_4 + g_{66}^2/c_{66}^{E})$ (Region II of Fig. 3). The stable FE solutions occur for $Q_x^2 = Q_y^2 = -\omega_M^2[V_4 + V_4' - (g_{66}^2/c_{66}^{E})]^{-1}$. From Eq. (4b), there are two solutions of different polarity for u_{xy} and P_z depending upon whether Q_{Mx} and Q_{My} have the same or opposite polarity. Externally induced switching between these sets of states accounts for the observed ferroelectric and ferroelastic properties. (Our free-energy expression reduces essentially to that of Ref. 5 for $Q_{Mx} = Q_{My} \equiv R$.[20])

Although symmetry arguments do not preclude terms of the form $P_z Q_{Mx} Q_{My}$ coupling the soft modes to the polarization, the absence of dielectric anomalies in a clamped crystal suggests that such terms are small, and that $P_s = P_z$ is produced indirectly through the piezoelectric term. This is, of course, the original argument of Cross, Fouskova, and Cummins,[3] but with the difference that we now see that u_s is itself, in turn, driven by the primary instability in the Brillouin zone boundary phonon.

We would like to thank Dr. L. Brixner for lending us the TMO crystal, and Dr. S. C. Abrahams for a preprint of unpublished work. It is a great pleasure to acknowledge several illuminating discussions with Professor W. Cochran. Finally, we thank Dr. E. Pytte for correspondence which restimulated our interest in these materials.

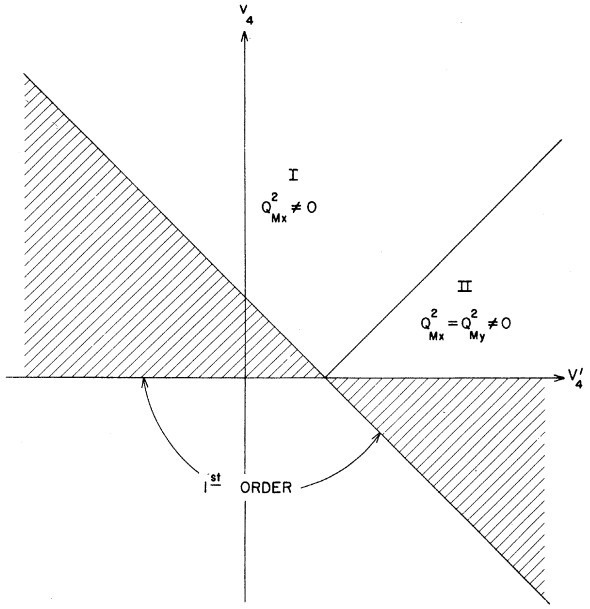

FIG. 3. The stable minimum of F given in Eq. (5) for $T < T_c$ depends upon the relative values of V_4 and V_4'. Region I exhibits a second-order transformation to a *non*ferroelectric phase; Region II, one to the FE phase of primary interest. In the cross-hatched regions either first- or second-order transformations are possible depending upon the nature of higher-order terms in F. In the remaining region only first-order transformations are possible.

---

*Work performed under the auspices of the U. S. Atomic Energy Commission.

†Guest scientist on leave from Institut für Festkörper und Neutronenphysik, Kernforschungsanlage-Jülich, Jülich, Germany.

[1]H. J. Borchardt and P. E. Bierstedt, J. Appl. Phys. 38, 2057 (1967).

[2]See, for example, S. E. Cummins, Ferroelectrics 1, 11 (1970); also A. W. Smith and G. Burns, Phys. Lett. 28A, 501 (1969).

[3]L. E. Cross, A. Fouskova, and S. E. Cummins, Phys. Rev. Lett. 21, 812 (1968).

[4]E. T. Keve, S. C. Abrahams, K. Nassau, and A. M. Glass, Solid State Commun. 8, 1517 (1970).

[5]E. Pytte, to be published.

[6]H. J. Borchardt and P. E. Bierstedt, Appl. Phys. Lett. 8, 51 (1966).

[7]R. E. Newnham, H. A. McKinstry, C. W. Gregg, and H. R. Stitt, Phys. Status Solidi 32, K49 (1969).

[8]L. A. Drobyshev, Yu. Ya. Tomashpolskii, A. I.

Safonov, G. N. Antonov, S. A. Fedulov, and Yu. N. Venevtsev, Kristallografiya 13, 1100 (1968) [Sov. Phys. Crystallogr. 13, 964 (1969)].

[9]J. Kvapil and V. John, Phys. Status Solidi 39, K15 (1970).

[10]The prominence of x-ray reflections corresponding to this smaller sublattice in the *lower* phase is particularly emphasized by E. T. Keve, S. C. Abrahams, and J. L. Bernstein, to be published.

[11]The incoming neutron energy was 14 meV (002), graphite monochromator and analyzer reflections, filtered to remove higher-order radiation. 20-min collimation was used before and after the sample.

[12]G. Shirane and Y. Yamada, Phys. Rev. 177, 858 (1969); J. D. Axe, G. Shirane, and K. A. Müller, Phys. Rev. 183, 820 (1969); V. J. Minkiewicz and G. Shirane, J. Phys. Soc. Jap. 26, 674 (1968).

[13]There is an additional small central component discernible at high temperatures. It is not yet certain whether it can be explained entirely by spurious effects. Further work is planned to elucidate this point.

[14]See, for example, W. Cochran, Advan. Phys. 18, 157 (1969).

[15]In practice, we used the plot of (T/I) in Fig. 1 to determine T_c and the high-temperature data to establish the proportionality between (T/I) and ω_M^2.

[16]L. D. Landau and E. M. Lifshitz, *Statistical Physics* (Pergamon, New York, 1958), pp. 430 ff.

[17]A. F. Devonshire, Advan. Phys. 3, 85 (1954).

[18]P. B. Miller and P. C. Kwok, Solid State Commun. 5, 57 (1967). Note that in order to emphasize the relation of the PE and FE phases, PE coordinates are used to describe the FE phase. In terms of the enlarged FE basis cell the condensed phonon has wave vector $\vec{q}=0$.

[19]It must be emphasized that Eq. (5) is deliberately truncated so as to display only the essential features of the reversible polarization and strain components of the FE phase. Other important terms and a discussion of the elastic and dielectric response are given in Ref. 5.

[20]The solution in Region I of Fig. 3 corresponds to a base-centered orthorhombic phase which is *non*polar since $Q_x Q_y = 0$. There seems to be no evidence for such a phase for RE molybdates. This solution is, however, rather closely related to the transformation which occurs in ADP ($NH_4H_2PO_4$).

Spontaneous-Fission Half-Life of ^{258}Fm and Nuclear Instability*

E. K. Hulet, J. F. Wild, R. W. Lougheed, J. E. Evans, and B. J. Qualheim
Lawrence Radiation Laboratory, University of California, Livermore, California 94550

and

M. Nurmia and A. Ghiorso
Lawrence Radiation Laboratory, University of California, Berkeley, California 94720
(Received 29 December 1970)

A spontaneous-fission activity decaying with a half-life of 380 ± 60 μsec, identified as ^{258}Fm, was discovered among the recoil products from the bombardment of ^{257}Fm with 12.5-MeV deuterons. The sharply decreasing spontaneous-fission lifetimes of nuclei with $N > 152$ show a determined trend contrary to theoretical predictions. The exceedingly short half-life of ^{258}Fm has led us to conclude that even-even nuclei in the immediate region beyond $N = 158$ are becoming catastrophically unstable toward fission.

As shown in Fig. 1, the spontaneous-fission half-lives of nuclei with neutron numbers greater than 152 decrease rapidly with increasing N (nuclei with more than 157 neutrons were unknown until now). Because of the perturbation introduced by the 152-neutron subshell, theoretical extrapolations of spontaneous-fission (SF) lifetimes for nuclei with neutron numbers above 156 are contradictory and allow the possibility of a recovery of stability at this level. Since theory was hopeful while the trend of experimental half-lives was pessimistic, it became important to search for an even-even nuclide well past the 152-neutron subshell.

Our search centered upon ^{258}Fm since we believed the fissionability of a nucleus containing 158 neutrons would not be influenced by the localized effect of the 152-neutron subshell. Thus, the SF half-life of ^{258}Fm would serve as an important guide to the nuclear stability of even heavier nuclei. We expected the principal mode of decay of ^{258}Fm to be spontaneous fission, since we estimated the SF half-life to be less than 2 h while systematics indicated a 70-200-day partial half-life for α decay.

Many experiments designed to identify ^{258}Fm were performed over a period of five years. Previously we made attempts to detect the spontaneous-fission decay of this nuclide in fermium chemically separated from the debris of thermo-